JOURNAL OF NANO- AND ELECTRONIC PHYSICS
Vol. **8** No 3, 03027(5pp) (2016)

ЖУРНАЛ НАНО- ТА ЕЛЕКТРОННОЇ ФІЗИКИ
Том **8** № 3, 03027(5cc) (2016)

Thickness-dependent Electrical and Piezoelectric Properties of Lead-Free Ferroelectric $Ba_{0.8}Sr_{0.2}TiO_3$ Thin Films

D.A. Kiselev[1,2,*], S.A. Levashov[2], M.S. Afanasiev[2], A.M. Kiselev[2], G.V. Chucheva[2]

[1] *National University of Science and Technology "MISiS", 4, Leninskiy pr., 119049 Moscow, Russia*
[2] *Kotelnikov Institute of Radio Engineering and Electronics Russian Academy of Sciences (Fryazino Branch), 1, pl. Vvedenskogo, Fryazino, 141190 Moscow region, Russia*

(Received 22 April 2016; published online 03 October 2016)

The thickness dependent of electrical and piezoelectric properties of lead-free ferroelectric $Ba_{0.8}Sr_{0.2}TiO_3$ thin films is reported. $Ba_{0.8}Sr_{0.2}TiO_3$ (BST 80/20) thin films for various thickness, ranging from 150 nm to 550 nm, were prepared by high-frequency reactive sputtering of a ceramic target in an oxygen atmosphere on *p*-type Si substrate. Memory windows and effective dielectric constant of the BST film in Au/BST/Si thin film capacitors is found to increase with the increasing thickness of the film. Domain structure, domain switching and hysteresis loops of the BST 80/20 thin film were investigate via the piezoresponse force microscopy. Complete domain switching and strong piezoresponse are found in the ferroelectric BST film. The piezoelectric coefficient (d_{zz}^{eff}) and the remnant piezoelectric response (ΔPR) of BST 80/20 films is found to increase with the thickness of the film.

Keywords: Lead-free ferroelectrics, Barium Strontium Titanate film, Polarization switching, Piezoelectric Force Microscopy

DOI: 10.21272/jnep.8(3).03027 PACS numbers: 68.55.jd, 77.22.Ch, 77.80.Dj, 68.37.Ps

1. INTRODUCTION

Currently ferroelectric thin films are widely used in the technique as piezoelectric transducers. Along with this, the discuss prospects of using ferroelectric materials in storage systems and elements microwave technology [1-3]. Ferroelectric barium strontium titanate (BST) thin films have been widely investigated as potential materials for the applications of microelectronic devices such as nonvolatile random access memories, infrared detectors, and microwave devices [4, 5, 6]. For these new applications, methods were developed and/or refined for depositing thin BST film by industry-standard and high-throughput techniques such as RF sputtering and Metal-organic Chemical Vapor deposition (MOCVD), and the electrical properties of the thin-films proved to be significantly different than bulk ceramics of the similar composition [7]. In addition, Queraltó et al. demonstrated the ability of the UV laser irradiation technique combined with the chemical solution deposition for fabricating tens of nanometers thick highly crystalline epitaxial BST/LNO/LAO films in a fast way [8]. The obtained films exhibit ferroelectric switching with perpendicular polarization comparable to similar systems produced by time-consuming conventional annealing methods. In Ref. [9] shown that multilayered ferroelectric BST films with a systematic variation in the composition (and thus the polarization) have a higher piezoelectric response compared to homogeneous samples for certain field magnitudes. The choice of the composition of a material of the ferroelectric $Ba_xSr_{1-x}TiO_3$ due to the fact that the composition has a pronounced hysteresis of polarization by an applied voltage [1]. Recently, the ferroelectric domain structure of BST 80/20 films grown on the MgO substrate and observed by the piezoresponse force microscopy depends significantly on their thicknesses [10]. Authors shown that films with thicknesses less than 36 nm contain only *aa* domains whose dimensions decrease with increasing film thickness. Films with thicknesses greater than 36 nm contain only c domains whose dimensions increase with increasing film thickness. At the same time for the BST 50/50 thin film when the film thickness increased from 90 to 170 nm, the average lateral grain size increased from 45 to 87 nm, and the dielectric permittivity of films increased from 650 to 1250, measured at 100 kHz and the room temperature [11]. In addition, it is important to understand how the film thickness affects electrical and ferroelectric properties, considering the ever-decreasing device size and the film thickness. In this paper, we have systematically studied the thickness effect on electrical, ferro- and piezoelectric properties of BST 80/20 films with the thickness between 150 nm and 550 nm, prepared by the high frequency reactive sputtering on the Si substrate with *p*-type conductivity in order to understand its functional properties for future flash memory applications.

2. EXPERIMENTAL DETAILS

The lead-free ferroelectric $Ba_{0.8}Sr_{0.2}TiO_3$ films 150-550 nm thick were prepared by the high-frequency reactive sputtering of a ceramic target in an oxygen atmosphere on the PLAZMA-50 SE setup as described elsewhere [12]. Following technological regimes were chosen for the growth of $Ba_{0.8}Sr_{0.2}TiO_3$ films: the oxygen pressure during sputtering was 60 ± 5 Pa; the distance between the target and a substrate was 10 ± 0.5 mm, the power of the high-frequency discharge was 230 ± 5 W; the substrate temperature was 605 ± 5 °C; the deposition time was from 5 min to 30 min. Under these conditions, the film growth rate was 15.0 nm/min.

* dm.kiselev@gmail.com

For measurements of electrical properties, dot-shaped Au top electrodes with an area of ~ 2.7×10^{-4} cm^2 were deposited on the surface of BST films using a shadow mask by the vacuum evaporation. Capacitance-voltage (C-V) characteristics were measured at room temperature on an automated experimental setup using the LCR Agilent E4980A precision tester. Dielectric properties of BST films were evaluated from C-V characteristics of fabricated capacitors metal-ferroelectric-semiconductor (MFS).

The surface morphology and the piezoelectric response of the BST 80/20 films were measured by the scanning probe microscopy Asylum MFP-3D in the Single Frequency Piezoresponse Force Microscopy mode (PFM) [13] and Dual AC Resonance Tracking PFM (DART-PFM) [14]. We used commercial probes ASYLEC-01 with titanium-iridium conductive coating with a curvature radius of $R = 28$ nm and the resonance frequency $f = 70$ kHz and the spring constant $k = 2$ N/m. Specifically, for the piezoelectric response (vertical piezoresponse – VPFM) measurement, the thin films were grounded with a conducting layer (p-type Si substrate) served as a back electrode grounded using a silver paste to the PFM stage. DC voltage of amplitude 40 V was applied between the tip and the ground electrode while the sample surface was scanned. After each poling scan, the same area was imaged in the PFM mode to see whether the PFM contrast was changed locally.

3. RESULTS AND DISCUSSIONS

The microstructure, such as average lateral grain size and a surface roughness, is one of the key parameters determining the electrical properties of the high dielectric thin film capacitor. Fig. 1(a) shown the cross-sectional view of the SEM image of the BST thin film. The thickness of the BST film was about 350 nm.

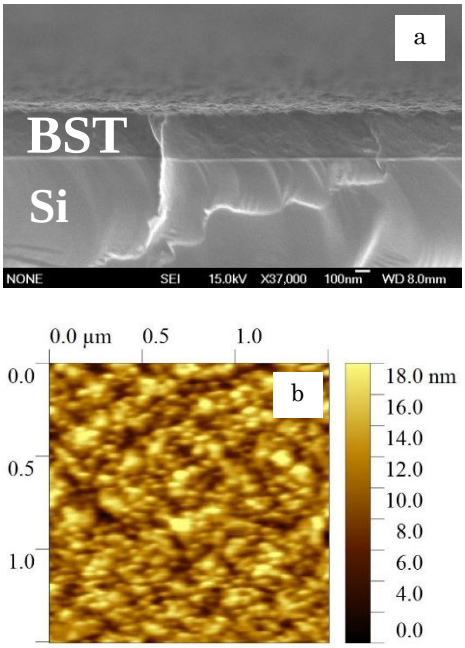

Fig. 1 – The cross-sectional view of the SEM image (a) and the 2D AFM topography image (b) of the BST 80/20 thin film

Fig. 1 (b) illustrate the atomic force microscopy image of the BST 80/20 thin film deposited at the optimum deposition conditions. The microstructure showed uniformly distributed grains. The average lateral grain size of the BST 80/20 film with thickness 350 nm was 40 nm, the root mean square (Rms) surface roughness measured over an area of 1.5 × 1.5 µm^2 was 2.8 nm. This procedure was made for all investigated thin films. Table 1 summarizes the statistical parameters for *as-grown* BST 80/20 films in the present work. As can see from the Table 1, without exception, parameters of R_{ms} and the lateral grain size increases with BST film thickness.

Table 1 – Root mean square (R_{ms}) surface roughness, lateral grain size obtained from atomic force microscopy images of BST 80/20 thin films for different thickness

Thickness (nm)	R_{ms} (nm)	Lateral grain size (nm)
150	1.5	31
250	2.3	34
350	2.8	40
450	3.6	52
550	4.9	65

Fig. 2 (a) shown a typically C-V curves of the MFS structures (Au/BST(350 nm)/Si) fabricated on p-type Si substrates at a frequency of 100 kHz. The bias voltage was varied from – 20 V to 20 V and back with the step 0.1 V. The C-V characteristics of the MFS capacitor shows a hysteresis loop with a counterclockwise rotation, which shows ferroelectric polarization switching type behavior.

This mode of switching is the desired mode for the memory operation. In addition, the C-V curve (Fig. 2(a)) shift right along the voltage axis for thicker films and do not show symmetrical with respect to zero voltage. This imprinted behavior may be resulted from the some fixed charge in the insulating layer.

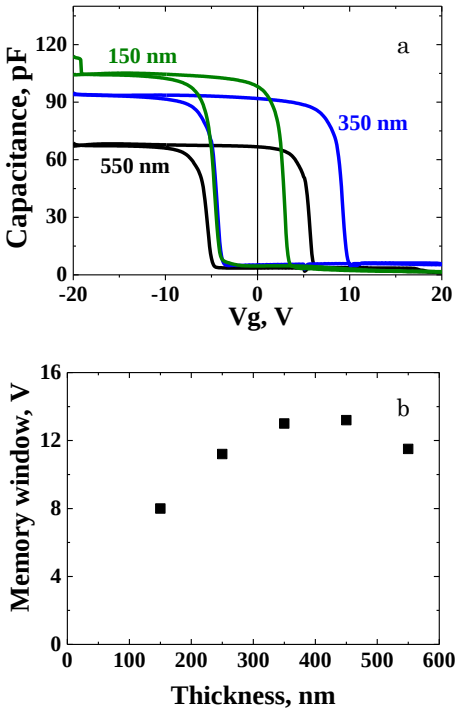

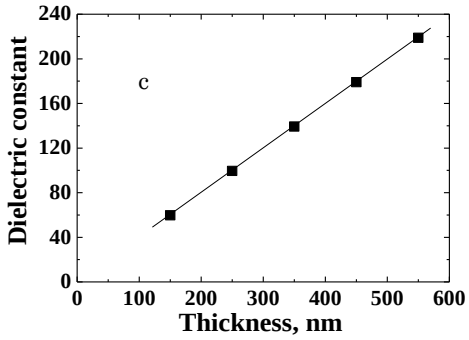

Fig. 2 – C-V characteristics of the Au/BST/Si (a), summary memory windows of the MFS (b) and the effective dielectric constant (c) of BST 80/20 thin films as a function of the film thickness

Also, a hysteresis in the C-V curve indicates a memory window related to a coercive field of the ferroelectric material [15]. Fig. 2 (b) summarizes the memory windows of the MFS structures as a function thickness of BST layer. The memory windows are determined with the difference of flatband voltages in the forward and reverse C-V curves. As can see from the data the memory windows increases with the increase of the BST film thickness and ultimately tends to a saturation. The effective dielectric constant of BST films used in the multilayered capacitor, Au/BST/Si, have a linear dependence from the BST film thickness (Fig. 2c). Results show that dielectric properties measured in the kHz range are strongly influenced by the grain size. The increase of the grain size with increasing of BST layer thickness coincides with the increase of permittivity, in agreement with the dielectric grain size effect. The tensile residual stress, which develops as a consequence of the thermal expansion mismatch between the substrate and the film, is high and increases with increasing thickness [11].

PFM images of the ferroelectric behavior of BST 80/20 350-thick film through DART-PFM as a response to the bias voltage (2 V_{AC}) at the room temperature as shown in Fig. 3(a-c). These figures consisted of the topography as well as the PFM amplitude and the PFM phase images, which reveal information about the local electromechanical response and the out-of-plane ferroelectric domain distribution.

Fig. 3(c) represents the results of the polarization reversal through local hysteresis loops on the BST 80/20 film deposited on the *p*-type Si substrate. The domain switching in two directions was successfully achieved.

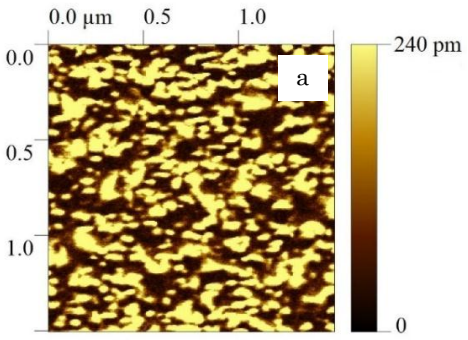

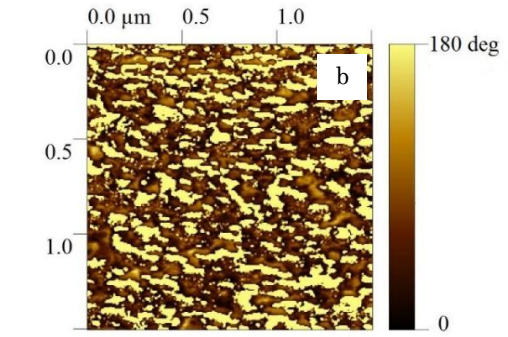

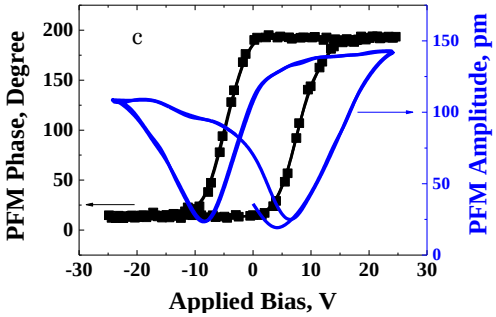

Fig. 3 – Piezoresponse force microscopy amplitude (a) and phase (b) images for BST 80/20 film 350 nm-thick. PFM hysteresis loops (c) – Phase and Amplitude signals vs Voltage

Fig.4 (a) shows piezoelectric hysteresis loops as a function of different thicknesses of the BST 80/20 film. The films present well-known butterfly curves for the variation of the VPFM amplitude versus the voltage. All the amplitude curves also confirm the existence of switchable intrinsic polarization in the BST 80/20 film.

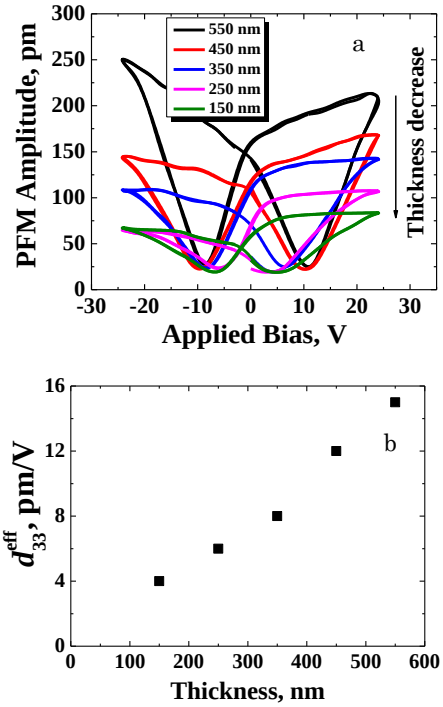

Fig. 4 – The local PFM amplitude hysteresis loops (a) for BST 80/20 thin films with different thickness and thickness-dependence effective piezoelectric coefficient d_{zz}

As can see from loops the value of maximum amplitude and the slope increased with increasing the BST layer thickness. The piezoelectric coefficient d_{zz}^{eff} was calculated from the slope of the linear region of the loop of the non-biased butterfly curves [16]. The thickness-dependent d_{zz}^{eff} of BST 80/20 films are presented in Fig. 4 (b). The effective piezoelectric coefficient d_{33} of the 150 nm thick BST film is about 4-5 pm/V, which has good agreement with the value obtained on the 130.5 thick BST film (3 pm/V) [17]. For BST 80/20 films observed an increase the value of effective piezoelectric constant d_{zz}^{eff} with the film thickness. This increase are due to the surface strain and the effect of interface between the ferroelectric and the substrate.

Ferroelectricity in all BST 80/20 thin films was investigated by vertical PFM and same. Again, as example, the Fig. 5(a) presents of the switching experiment on the *as-grown* BST 80/20 thin film with thickness 350 nm. For all BST films, local poling was successful by applying ± 40V DC while scanning a area of 10 × 10 μm^2 which created a strong bright (left side at + 40 V) and dark (right side at – 40 V) contrast in VPFM image. Small remark, we removed offset for all VPFM images for better image clarity. However, our recent experimental results on piezoelectric response of BST 80/20 films [4] indicate that the BST film have self-polarization effect, in the current paper this effect not discussed.

Fig. 5(b) shown the cross-sectional data of the piezoresponse signal changes across the center PFM image include a as-grown state and poling area. From this graph, we calculate the average remnant piezoresponse signal (ΔPR) as is difference between the amplitude for positive and negative poling areas. For the BST 80/20 film with thickness 350 nm a value ΔPR = 780 pA. Thus, we have defined values ΔPR for all investigate

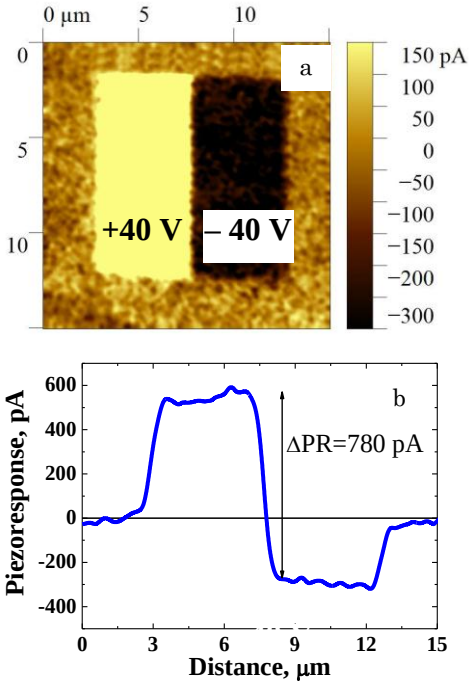

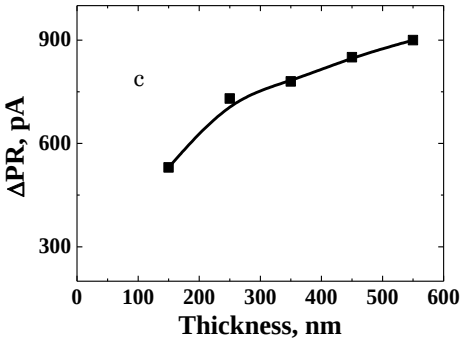

Fig. 5 – The piezoresponse image (a) obtained by applying a DC bias voltage (positive and negative) to the BST 80/20 film and the cross-section profile (b) of the piezoresponse signal along a center scan in (a). Remnant PFM signal (c) as a function of film thickness

BST thin films with different thickness; Fig. 5(c) summarizes this data.

Increasing a value of the remnant piezoresponse with the thickness of the BST film confirm result observe d_{zz}^{eff} for these films (Fig. 4 and Fig. 5(c)). Similar phenomena are observed in the ultrathin $BiFeO_3$ films grown on STO (001) substrate with a $La_{0.67}Sr_{0.33}MnO_3$ cover layer [18] and in epitaxial PZT ultrathin films 50–500 Å thick grown on SRO buffered (100) STO substrate by pulsed laser deposition [19], where it was shown, that this apparent contradiction between the structural measurements and the measured switchable polarization is explained by an increasing presence of a strong depolarization field, which creates a pinned 180° polydomain state for the thinnest films.

4. CONCLUSIONS

In summary, polycrystalline $Ba_{0.8}Sr_{0.2}TiO_3$ thin films with thickness ranging from 150 nm to 550 nm were prepared by the RF magnetron sputtering. AFM illustrated that the deposition time or thickness had an influence on the surface morphology and latera grain sizes of BST 80/20 films. The MFS structure (Au/BST/Si) showed hysteretic characteristics in the C-V plot with a typical window memory, and this parameter depended from the film thickness. Increasing the thickness would result in an increase in the dielectric constant, which mainly stems from dielectric grain size effect and the interfacial-layers effect. The piezoelectric coefficient (d_{zz}^{eff}) and the remnant piezoelectric response (ΔPR) of BST 80/20 films is found to increase with the increasing thickness of the film. Our studies on ferroelectric BST 80/20 thin films therefore indicate that although ferroelectricity is maintained down to hundred nanometer level thickness, switchable polarization (value of ΔPR) is severely affected.

ACKNOWLEDGEMENT

The studies are performed on the equipment of Center for Shared Use "Materials Science and Metallurgy" at the National University of Science and Technology "MISiS". The study was supported in part by the Russian Foundation for Basic Researches (projects 16-07-00665 and 16-07-00666).

REFERENCES

1. Yu.V. Gulyaev, A.S. Bugaev, A.Yu. Mityagin, G.V. Chucheva, M.S. Afanasev, *Achievements of Modern Radioelectronics* **12**, 3 (2011).
2. K.A. Vorotilov, A.S. Sigov, A.A. Romanov, P.R. Mashevich, *Nanotechnology: development and applications - XXI century* 4, 4 (2012).
3. K.A. Vorotilov, A.S. Sigov, *Phys. Solid State* **54**, 894 (2015).
4. D.A. Kiselev, M.S. Afanasiev, S.A. Levashov, G.V. Chucheva, *Phys. Solid State* **57**, 1151 (2015).
5. F.M. Pontes, E.R. Leite, D.S.L. Pontes, *J. Appl. Phys.* **91**(9), 5972 (2002).
6. K. Nadaud, C. Borderon, R. Gillard, E. Fourn, R. Renoud, H. W. Gundel, *Thin Solid Films* **591**, 90 (2015).
7. C. Basceri, S.K. Streiffer, A.I. Kingon, R. Waser, *J. Appl. Phys.* **82**(5), 2497 (1997).
8. A. Queraltó, A. Pérez del Pino, M. de la Mata, J. Arbiol, M. Tristany, A. Gómez, X. Obradors, T. Puig, *Appl. Phys. Lett.* **106**, 262903 (2015).
9. R. Nath, S. Zhong, S.P. Alpay, B.D. Huey, M.W. Cole, *Appl. Phys. Lett.* **92**, 012916 (2008).
10. A.N. Kuskova, R.V. Gainutdinov, O.M. Zhigalina, *Journal of Surface Investigation. X-ray, Synchrotron and Neutron Techniques* **8**(4), 791 (2014).
11. T. Pečnik, S. Glinšek, B. Kmet, B. Malič, *J. Alloy. Compd.* **646**, 766 (2015).
12. M.S. Ivanov, M.S. Afanas'ev, *Phys. Solid State* **51**(7), 1328 (2009).
13. A. L. Gruverman, J. Hatano, H. Tokumoto, *Jpn. J. Appl. Phys. Part 1* **36**(4A), 2207 (1997).
14. B. J. Rodriguez, C. Callahan, S. V. Kalinin, R. Proksch, *Nanotechnology* **18**(47), 475504 (2007).
15. K. Uda, T. Kijima, *The Rigaku Journal* **17**(2), 45 (2000).
16. Y. Bai, J. Chen, R. Tian, S. Zhao, *Mater. Lett.* **164**, 618 (2016).
17. S.R. Kwon, W. Huang, L. Shu, F.-G. Yuan, J.-P. Maria, X. Jiang, *Appl. Phys. Lett.* **105**, 142904 (2014).
18. J.L. Zhao, H.X. Lu, J.R. Sun, B.G. Shen, *Physica B* **407** 2258 (2012).
19. V. Nagarajan, J. Junquera, J.Q. He, C.L. Jia, R. Waser, K. Lee, Y.K. Kim, S. Baik, T. Zhao, R. Ramesh, Ph. Ghosez, K.M. Rabe, *J. Appl. Phys.* **100**, 051609 (2006).